ELSEVIER

Journal of Materials Processing Technology 182 (2007) 333–342

Journal of Materials Processing Technology

www.elsevier.com/locate/jmatprotec

Simulation of EPS foam decomposition in the lost foam casting process

X.J. Liu [a,*], S.H. Bhavnani [b,1], R.A. Overfelt [c,2]

[a] *United States Steel Corporation, Great Lakes Works, #1 Quality Drive, Ecorse, MI 48229, United States*

[b] *213 Ross Hall, Department of Mechanical Engineering, Auburn University, Auburn, AL 36849-5341, United States*

[c] *202 Ross Hall, Department of Mechanical Engineering, Materials Engineering Program, Auburn University, Auburn, AL 36849-5341, United States*

Received 17 April 2006; received in revised form 14 July 2006; accepted 21 August 2006

Abstract

The importance of smooth mold filling in the lost foam casting (LFC) process has been recognized for a long time. The more uniform the filling process, the better the quality of the casting products that are produced. Successful computer simulations can help to reduce the number of trials and cut down the lead time in the design of new casting products by better understanding the complex mechanisms and interplay of different process parameters in the mold filling process. In this study, a computational fluid dynamics (CFD) model has been developed to simulate the fluid flow of molten aluminum and the heat transfer involved at the interfacial gap between the metal and the expanded polystyrene (EPS) foam pattern. The commercial code FLOW-3D was used because it can track the front of the molten metal by a Volume of Fluid (VOF) method and allow complicated parts to be modeled by the Fractional Area/Volume Ratios (FAVOR) method. The code was modified to include the effects of varying interfacial heat transfer coefficient (VHTC) based on gaseous gap pressure that is related to foam degradation and coating permeability. The modification was validated against experimental studies and the comparison showed better agreement than the basic constant heat transfer (CHTC) model in FLOW-3D. Metal front temperature was predicted within experimental uncertainty by the VHTC model. Mold filling patterns and filling time difference of 1–4 s, were more precisely captured by the VHTC model than the CHTC model for several geometries. This study has provided additional insight into the effect of important process and design variables in what has traditionally been a very empirical field.

Keywords: Lost foam casting; Heat transfer coefficient; Gas pressure; VOF-FAVOR

1. Introduction

In the last two decades the lost foam casting (LFC) process has been widely adopted to manufacture complex parts without the need for cores. This is particularly true in the aluminum casting industry because automotive manufacturers currently produce a wide range of engine blocks and cylinder heads with LFC technology. The basic procedures, application and advantages can be found in [1]. The LFC process has mainly been developed based on the empirical knowledge of experienced practitioners. Numerical modeling of expanded polystyrene (EPS) foam decomposition is only recently reaching a point where it can provide useful insight in helping optimize design and process variables.

In the LFC process, an expanded polystyrene foam pattern of the desired shape is placed in a sand mold with appropriate gating systems. The foam pattern undergoes collapse, melting, vaporization, and degradation when the molten metal front advances into the pattern. A kinetic zone, which is the gap between the advancing metal front and the receding foam pattern, has been proposed by Warner et al. [2] to model the LFC process. During the mold filling process, the degradation products escape from the kinetic zone through the coating layer into the sand. Complex reactions between the molten metal and foam pattern make the simulation of the LFC process extremely difficult.

The simulation of traditional sand casting with an empty mold has been studied extensively since the SOLution Algorithm-Volume of Fluid (SOLA-VOF) method was first formulated by Hirt and Nichols [3]. Due to the fact that the lost foam casting process shares many characteristics with the traditional sand casting, the theory and techniques applied to model this new

* Corresponding author. Tel.: +1 313 749 3566; mobile: +1 313 402 6238; fax: +1 313 749 3651.

E-mail addresses: xliu@uss.com (X.J. Liu), bhavnsh@auburn.edu (S.H. Bhavnani), overfra@auburn.edu (R.A. Overfelt).

[1] Tel.: +1 334 844 3348; fax: +1 334 844 3303.

[2] Tel.: +1 334 844 5940; fax: +1 334 844 3400.

0924-0136/$ – see front matter © 2006 Elsevier B.V. All rights reserved.
doi:10.1016/j.jmatprotec.2006.08.023

process mostly originated from simulation methods developed for traditional sand casting. By assuming that the pattern decomposition rate is a linear function of metallostatic head and metal front temperature, Wang et al. [4] simulated the lost foam casting process in complex 3D geometries based on the existing computer program of conventional sand casting. Liu et al. [5] included back pressure in the kinetic zone with a simple 1D mathematical model to predict metal front velocity. Mirbagheri et al. [6] developed a foam degradation model with a pressure correction scheme for the free surface at the metal front based on the SOLA-VOF technique. A similar backpressure force scheme was adopted by Kuo et al. [7] in the momentum equation and the value of this force was adjusted to study the filling sequence of patterns according to experimental results.

Most of these simulations successfully predict a much slower filling speed for LFC process than that of traditional sand casting process. But the role of foam degradation is mostly not a part of the models and experimental data or empirical functions are needed to perform simulations. The present study modifies the basic LFC model in commercial code FLOW-3D, which uses a constant heat transfer coefficient (CHTC), to include the effects of varying heat transfer coefficient (VHTC) based on gaseous gap pressure which is related to foam degradation and coating permeability. The modification was validated against experimental studies for several process variables.

Additionally, defect formation that is the most important issue with lost foam casting, is not modeled in the numerical work cited from literature. Pyrolysis defects such as folds, internal pores and surface blisters account for a large amount of scrap in LFC operations. The defect prediction capability of FLOW-3D is very important to understand and optimize the process.

2. Mathematical and numerical model

2.1. Governing equations

The fluid flow of molten metal during mold filling is characterized by a transient condition with a moving surface. The mathematical model includes the continuity, momentum and energy equations in the molten metal, moving metal front and porous wall boundary conditions. The governing equations can be described as follows.

(a) Mass continuity equation:

$$\frac{\partial}{\partial x}(uA_x) + R\frac{\partial}{\partial y}(vA_y) + \frac{\partial}{\partial z}(wA_z) + \xi\frac{uA_x}{x} = 0 \tag{1}$$

where the velocity components (u, v, w) are in the coordinate directions (x, y, z) or (r, θ, z); A_x is the fractional area open to flow in the x direction, A_y and A_z are similar area fractions for flow in the y and z directions, respectively. The coefficient R depends on the choice of coordinate system as described in FLOW-3D user's manual [8]. When cylindrical coordinates are used, y derivatives are converted to azimuthal derivatives,

$$\frac{\partial}{\partial y} \rightarrow \frac{1}{r}\frac{\partial}{\partial \theta} \tag{2}$$

In FLOW-3D code, this transformation is accomplished by using the equivalent form

$$\frac{1}{r}\frac{\partial}{\partial \theta} = \frac{r_m}{r}\frac{\partial}{\partial \theta} \tag{3}$$

where $y = r_m$, θ and r_m is a fixed reference radius. When Cartesian coordinates are used, R is set to unity and ξ is set to zero.

(b) Momentum equations:

$$\frac{\partial u}{\partial t} + \frac{1}{V_f}\left\{uA_x\frac{\partial u}{\partial x} + vA_yR\frac{\partial u}{\partial y} + wA_z\frac{\partial u}{\partial z}\right\} - \xi\frac{A_yv^2}{xV_f} = -\frac{1}{\rho}\frac{\partial P}{\partial x} + G_x + F_x \tag{4}$$

$$\frac{\partial v}{\partial t} + \frac{1}{V_f}\left\{uA_x\frac{\partial v}{\partial x} + vA_yR\frac{\partial v}{\partial y} + wA_z\frac{\partial v}{\partial z}\right\} + \xi\frac{A_yuv}{xV_f} = -\frac{1}{\rho}R\frac{\partial P}{\partial y} + G_y + F_y \tag{5}$$

$$\frac{\partial w}{\partial t} + \frac{1}{V_f}\left\{uA_x\frac{\partial w}{\partial x} + vA_yR\frac{\partial w}{\partial y} + wA_z\frac{\partial w}{\partial z}\right\} = -\frac{1}{\rho}\frac{\partial P}{\partial z} + G_z + F_z \tag{6}$$

where (G_x, G_y, G_z) are body acceleration (forces per unit mass), (F_x, F_y, F_z) are viscous forces per unit mass, V_f is the fractional volume open to flow, and ρ is the density of molten metal.

(c) Fluid energy equation:

$$V_f\frac{\partial}{\partial t}(\rho I) + \frac{\partial}{\partial x}(\rho IuA_x) + R\frac{\partial}{\partial y}(\rho IvA_y) + \frac{\partial}{\partial z}(\rho IwA_z) + \xi\frac{\rho IuA_x}{x} = \mathrm{TDIF} \tag{7}$$

where I is the macroscopic mixture internal energy; TDIF is the heat diffusion term

$$\mathrm{TDIF} = \frac{\partial}{\partial x}\left(kA_x\frac{\partial T}{\partial x}\right) + \frac{\partial}{\partial y}\left(kA_y\frac{\partial T}{\partial y}\right) + \frac{\partial}{\partial z}\left(kA_z\frac{\partial T}{\partial z}\right) + \xi\frac{kA_xT}{x} \tag{8}$$

where k is the thermal conductivity of the fluid.

2.2. Computational features of FLOW-3D

SOLA-VOF has been widely used in simulation of all types of casting problems, and it has been shown to be more effective in solving transient moving surface problems [9]. FLOW-3D also uses this methodology to solve the governing equations of the LFC process with adjustable time steps to improve efficiency, accuracy and stability. The numerical solutions of the governing equations are approximated by finite difference methods. The momentum Eqs. (4)–(6) are discretized as follows.

$$u_{i,j,k}^{n+1} = u_{i,j,k}^{n} + \delta t^{n+1}\left[-\frac{p_{i+1,j,k}^{n+1} - p_{i,j,k}^{n+1}}{(\rho\delta x)_{i+(1/2),j,k}^{n}}\right] + G_x - \mathrm{FUX} - \mathrm{FUY} - \mathrm{FUZ} + \mathrm{VISX} - \mathrm{WSX} \tag{9}$$

$$v_{i,j,k}^{n+1} = v_{i,j,k}^{n} + \delta t^{n+1}\left[-\frac{p_{i,j+1,k}^{n+1} - p_{i,j,k}^{n+1}}{(\rho\delta y)_{i,j+(1/2),k}^{n}}\right] R_{i+(1/2)} + G_y - \mathrm{FVX} - \mathrm{FVY} - \mathrm{FVZ} + \mathrm{VISY} - \mathrm{WSY} \quad (10)$$

$$w_{i,j,k}^{n+1} = w_{i,j,k}^{n} + \delta t^{n+1}\left[-\frac{p_{i,j,k+1}^{n+1} - p_{i,j,k}^{n+1}}{(\rho\delta z)_{i,j,k+(1/2)}^{n}}\right] + G_z - \mathrm{FWX} - \mathrm{FWY} - \mathrm{FWZ} + \mathrm{VISZ} - \mathrm{WSZ} \quad (11)$$

where n stands for different time levels, and i, j and k are space cells. FUX is the advective flux of u in the x direction, VISX is the x-component viscous acceleration, WSX is the viscous wall acceleration in the x direction, and GX is gravitational force. The y and z components have similar meanings. All these forces except the advective flux are discretized by centered difference. $R_{i+(1/2)}$ is used to convert between the Cartesian and cylindrical coordinates, which equals one for Cartesian coordinate and equals $2x_{\max}/(x_i + x_{i+1})$ for cylindrical coordinate. The modified donor-cell method is used to weigh the upstream quantity more than downstream to obtain higher order of accuracy and save computational time.

$$\mathrm{FUX} = \frac{0.5}{\mathrm{VFC}}[(\mathrm{UAR} - \alpha|\mathrm{UAR}|)\mathrm{DUDR} + (\mathrm{UAL} + \alpha|\mathrm{UAL}|)\mathrm{DUDL}] \quad (12)$$

where

$$\mathrm{DUDL} = \frac{u_{i,j,k} - u_{i-1,j,k}}{\delta x_i} \quad (13)$$

$$\mathrm{DUDR} = \frac{u_{i+1,j,k} - u_{i,j,k}}{\delta x_{i+1}} \quad (14)$$

$$\mathrm{UAR} = 0.5(u_{i+1,j,k}AFR_{i+1,j,k} + u_{i,j,k}AFR_{i,j,k}) \quad (15)$$

$$\mathrm{UAL} = 0.5(u_{i,j,k}AFR_{i,j,k} + u_{i-1,j,k}AFR_{i-1,j,k}) \quad (16)$$

and

$$\mathrm{VFC} = \frac{(\delta x_i VF_{i,j,k} + \delta x_{i+1} VF_{i+1,j,k})}{(\delta x_i + \delta x_{i+1})} \quad (17)$$

where AFR is fractional area A_x for flow in x direction at cell face, and VF is fractional volume for flow at the center of cell (i, j, k). The basic idea of Eq. (12) is to weigh the upstream quantity by a factor of $(1+\alpha)$ and down stream by $(1-\alpha)$ resulting in higher order of accuracy for the discretization scheme [8].

In the SOLA-VOF method, there are seven basic steps for the solution algorithm as follows.

Step 1: Assign initial pressure field.
Step 2: Compute velocity field from momentum equation by Eq. (9)–(10).
Step 3: Solve Poisson equation resulted from the continuity equation to calculate pressure change for molten metal flow field, and find velocity based on metal front model for foam-metal interface.
Step 4: Correct pressure and velocity due to change in pressure.
Step 5: Repeat Step 3 and 4 until continuity is satisfied.
Step 6: Update remaining variables using new velocities.
Step 7: Move to next time cycle until desired time interval is reached.

Apart from the basic implementation of the SOLA-VOF algorithm, an advantageous Fractional Area/Volume Ratios (FAVOR) method was selected as the basis of FLOW-3D. With this method, complex flow regions can be simulated with structured, smoothly varying, fast to generate, and strictly orthogonal grids with comparable accuracy of body-fitted coordinate (BFC) methods. However, constructing good quality BFC grids is very difficult and time-consuming to establish workable grids. The FAVOR method combined with SOLA-VOF algorithm allows the use of coarser grids and improves the accuracy of the numerical solutions for complex geometries and fluid surface tracking.

2.3. Basic model of metal front velocity with gravity effect

Flow of molten metal in the LFC casting process is different from traditional sand casting because of the boundary conditions at the metal front. The free surface condition usually used in traditional sand casting needs to be modified in simulating the LFC process because of the existence of foam patterns in front of molten metal instead of air or a void in traditional sand casting. The boundary conditions at the wall also need to incorporate the effect of coating materials outside of the foam pattern.

The metal front velocity is a function of the heat absorbed by the foam, which depends not only on the properties of EPS foam and molten metal, but also on process variables such as temperature of the metal, pressure head, pattern coating materials, and orientation of gravity. To find the metal front velocity, let q_s be the heat transfer rate from metal front to the kinetic zone [10]. Then from Newton's Law of Cooling, we have

$$q_s = h(T_s - T_z)A_c \quad (18)$$

where h is the heat transfer coefficient at the metal front, T_s is the metal front surface temperature, T_z is the kinetic zone temperature, and A_c is the cross-section area of metal front. The energy required by the foam pattern to get liquefied, vaporized and depolymerized can be expressed as

$$q_f = \dot{m}c_p(T_s - T_z) + \dot{m}Q_{liq} + \dot{m}Q_{vap} + \dot{m}Q_{depoly} \quad (19)$$

where q_f is the surface heat flux to foam pattern, c_p is the EPS foam specific heat, Q_{liq} is the latent heat of fusion of foam, Q_{vap} is the heat of vaporization, Q_{depoly} is the heat of depolymerization, and the mass flow rate is

$$\dot{m} = \rho A_c V_{adv} \quad (20)$$

where ρ is the EPS foam density, and V_{adv} is the metal front advancing velocity. An energy balance can be applied between q_s and q_f to find the metal front advancing velocity,

$$V_{adv} = \frac{h(T_s - T_z)}{\rho(c_p(T_s - T_z) + Q_{liq} + Q_{vap} + Q_{depoly})} \quad (21)$$

The treatment of the moving boundary conditions at the metal front is the most critical part of all the models of the LFC process. FLOW-3D uses a velocity approach, which is based on a heat transfer coefficient model as shown in Eq. (21). The model can also incorporate the effect of gravity orientation; a recent X-ray based study has confirmed that an upward moving front progresses more slowly than a downward moving front [11].

The gravity effect is taken into account by a correction factor, which is a function of gravity component normal to the metal/foam front. Because the foam decomposition products are lighter than the molten metal, the foam products can be displaced by the metal moving along the gravity direction and accumulate above the metal front that is moving against gravity direction. In FLOW-3D a correction factor used as a multiplier on the heat transfer coefficient is defined as

$$f_g = 1.0 + \text{sign}(g_{ht}) c_g \left(\frac{V_g}{V_g + V_{ht}} \right) \quad (22)$$

where g_{ht} is the gravity component normal to metal/foam front, c_g is a problem dependent factor, which can be tuned to improve agreement with data, and V_{ht} is the nominal velocity of the metal front, which is

$$V_{ht} = \frac{h}{\rho c_p} \quad (23)$$

V_g is the characteristic speed of gravity waves, which is defined as

$$V_g = \sqrt{|g_{ht}| r_s} \quad (24)$$

where r_s is the characteristic length scale of the surface irregularities at the metal/foam interface. A value of 0.1 cm for r_s is recommended in FLOW-3D user's manual [8].

2.4. Model with varying heat transfer coefficient

2.4.1. Effect of gas pressure

The pressure of gas produced by the foam plays an important role in the LFC process because it affects the metal filling behavior. Mirbagheri et al. [6] used empirical pressure equation to correct the free surface pressure originated from the application of the VOF method [3]. By forcing the tangential stress at the metal front to vanish and normal stress to balance the externally exerted normal stress, Kuo et al. [7] applied back pressure force in the momentum equation and used several trials to determine a proper back-pressure for the model to get agreement results with experimental data. In the current modeling study with FLOW-3D, a correction factor caused by the gas pressure at the metal front is introduced, as follows

$$f_p = c_k + (1 - c_k) \left(\frac{p_h}{p_h + p_g t_c} \right) \quad (25)$$

where c_k is the pressure coefficient, p_h is the average pressure head for the pouring of metal in the sprue, p_g is the gas pressure in the kinetic zone, and t_c is the ratio of coating thickness to the characteristic length scale of the surface irregularities r_s at the metal/foam interface.

The gas pressure in the kinetic zone is a value measured from experiments. It is dependent on many process variables, such as metal front velocity, foam density, metal temperature, coating permeability and thickness [12]. Under a typical metal front velocity of 1.5 cm/s, foam density of 24 kg/m^3 and coating thickness of 0.7 mm for aluminum LFC process, the gas pressure in the kinetic zone is reported to be 10–30 kPa [13].

2.4.2. Effect of metal temperature

Wang et al. [4] used a foam decomposition model in which the metal front velocity is a linear function of metal temperature. But from Yao's [14] experiment, the highest metal front velocity is observed at metal temperature of 490 °C. Metal temperatures less or higher than 490 °C lead to longer mold filling times. The non-linear dependency of metal front velocity on the metal temperature is probably related to the foam degradation characteristics. From Yao's analysis of foam degradation characteristics, the peak volatilization temperature for EPS foam is about 400–420 °C. If the metal temperature is less than the EPS peak volatilization temperature, the degradation products are essentially viscous residues, which may result in higher resistance to the flow molten metal and lower metal front velocity. At the EPS peak volatilization temperature, the gaseous degradation products consist essentially of the monomer. If the metal temperature is higher than the EPS foam peak volatilization temperature, the monomer molecules undergo extensive fragmentation and the volume of the gases produced increases resulting in higher pressure in the kinetic zone. The metal front velocity is also affected by the properties of the coating such as permeability and thickness. Depending on how effective the gaseous product can be eliminated through the coating layer of the foam pattern, the metal front velocity is reduced at different levels. The temperature effect is not modeled in the basic CHTC model of FLOW-3D. A correction factor was introduced to take into account the different metal pouring temperatures in the VHTC model of the current work.

$$f_T = c_T \left(\frac{T_p}{T_p + \text{abs}(T_m - T_p)} \right) \quad (26)$$

where T_p is the peak volatilization temperature set at 490 °C in this model, T_m is the metal pouring temperature, and c_T is a temperature coefficient. Values of c_T used for the simulation are listed in Table 1.

2.5. Model of defect tracking

The LFC model in FLOW-3D also provides a scheme to predict defects, which may originate from meeting of two fluid

Table 1
Coefficient of temperature for different metal temperature

Metal temperature (°C)	c_T
190	0.7
490	1.4
715	1.2
1115	1.0

fronts and by surface turbulence at the metal front [15]. The probability of defects is represented by a scalar variable that is initially zero in the flow region. The scalar quantity is incremented by an amount proportional to the mass of degraded foam in the control volume and it is allowed to accumulate at the metal front and to be trapped in metal if the two fronts meet. As the metal continues to fill the mold, the scalar variable can advect and diffuse into the casting. A second scalar quantity is introduced to account for the wicking of defect material into the coating and sand. This scalar can only gain defect material from the original defect scalar. Once the defect material is stuck to the walls, it does not move with the flowing metal and the quantity is taken out of the original scalar defect quantity. The wicking scalar is proportional to the product of the original defect scalar and the coating wall area located in that cell. A constant of proportionality coefficient, which is a rate per unit time and unit area is introduced and it is determined from experiment [16]. In the output of the simulation, the distribution of the scalar shows the probability of the defect formation locations.

3. Results and discussions

The proposed VHTC model was first validated against three experimental studies from the literature with geometries shown in Fig. 1. Parameters that were compared with experiments were metal front temperature and mold filling times. Then the VHTC model was used to predict the effect of gating system on defect formation of castings. Aluminum alloy 319 (Si = 6%, Cu = 3.5%) was used for all the problems. The thermophysical properties of aluminum 319 are listed in Table 2 [17].

3.1. Grid independence study

A cylindrical geometry is chosen to verify the VHTC model. The EPS foam pattern is 8.8 cm in diameter and 25.4 cm long. These dimensions were chosen because they match the size of patterns used in experimental studies [10,13] by the authors. The computational domain is shown in Fig. 1(a), where $h = 25.4$ cm and $r_0 = 4.4$ cm. At $r = 0$, a symmetric boundary condition was applied. A pressure boundary condition was used at the inlet, and no-slip boundary conditions were applied at the right and bottom walls. In order to determine the proper grid size for this study, a grid independence test was conducted for the cylindrical foam geometry. Four different grid densities $5^r \times 30^z$, $10^r \times 60^z$, $15^r \times 90^z$ and $20^r \times 120^z$ were used for the grid independence study. The integrated value of mass flow rate from the top gate, which reveals the accumulated effect of discretization error, is used as a monitoring measure of the accuracy of the solution. Fig. 2 shows the dependence of mass flow rate on the grid size of longitudinal direction. A similar trend is obtained on the grid in the radial direction. Comparison of the predicted value of mass flow rate among four different cases suggests that the grid distributions of $15^r \times 90^z$ and $20^r \times 120^z$ give nearly identical results. The relative change in mass flow rate is less than 0.5% between the grid densities of $15^r \times 90^z$ and $20^r \times 120^z$.

Since the FAVOR method is used in the geometry formation in the code, even the coarse grid $5^r \times 30^z$ results in a comparatively small difference of 1.5% from the finer grids. The benefit of using the FAVOR method to represent a complex geometry is very significant since accurate results can be obtained even with a coarse grid. This leads to great savings in computational time in simulations for complex geometries. Similar grid independence

Table 2
Thermophysical properties of aluminum alloy 319 [17]

Property	Value
Liquid metal density (kg/m^3)	2500
Solid metal density (kg/m^3)	2700
Thermal conductivity of liquid metal (W/m K)	79
Thermal conductivity of solid metal (W/m K)	145
Specific heat of liquid metal (J/kg K)	1145
Specific heat of solid metal (J/kg K)	963
Solidus temperature (°C)	450
Liquidus temperature (°C)	596
Viscosity (Pa s)	0.0016
Thermal expansion coefficient (1/K)	3.0E−5
Critical solidification fraction above which metal has no fluidity	0.51
Coefficient of solidification drag (1/s)	0.1

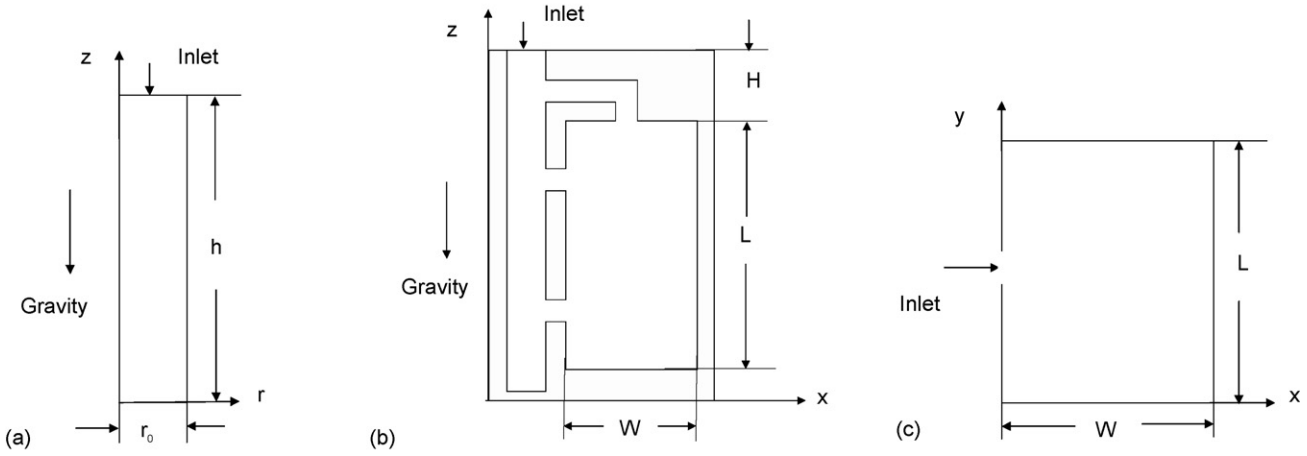

Fig. 1. Computational domains: (a) cylinder; (b) plate with three ingates; and (c) plate with side ingate.

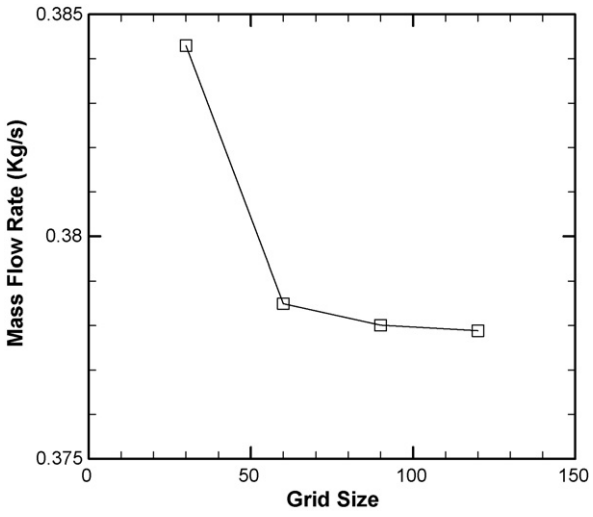

Fig. 2. The mass flow rate at the entrance of ingate as a function as the computational grid size.

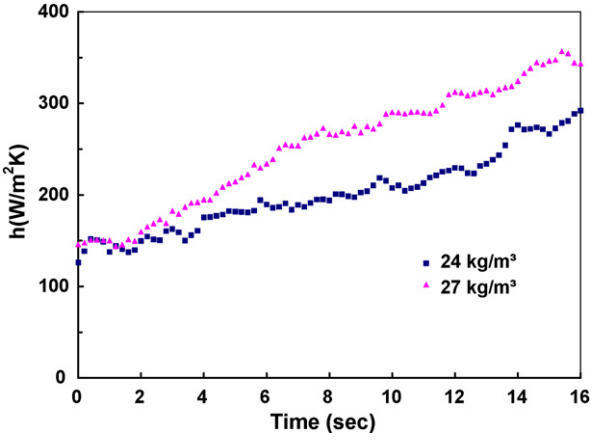

Fig. 3. Measured heat transfer coefficient between the metal front and foam pattern for a metal front velocity of 1.5 cm/s with coating thickness of 0.07 cm for two different foam densities.

studies were performed for the other geometries. Considering both accuracy and computational time, all the calculations were performed with grids that produce less than 1% difference from the finer grids.

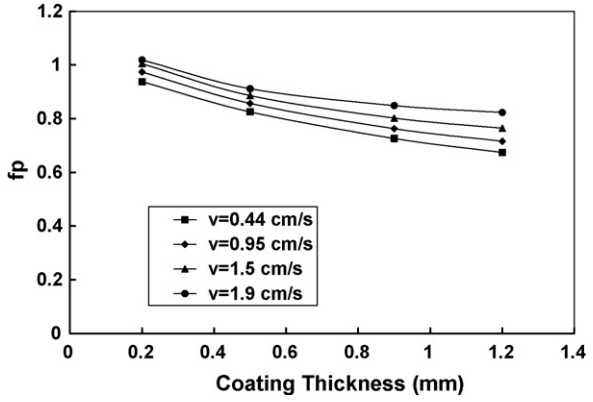

Fig. 4. Relation between correction factor of gas pressure and coating thickness.

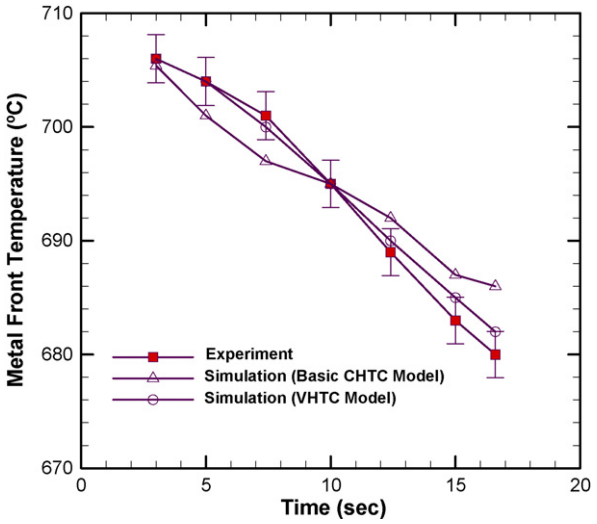

Fig. 5. Experimental validation of basic CHTC model and VHTC model.

3.2. Experimental validation

The simulation solutions are further validated with experimental data from [10], conducted by the present authors. From the experiment, it is found that the heat transfer coefficient increases as the metal front advances. Typical measured values of heat transfer coefficient for a metal front velocity of 1.5 cm/s with coating thickness of 0.07 cm for two different foam densities are shown in Fig. 3. In the VHTC model with gas pressure

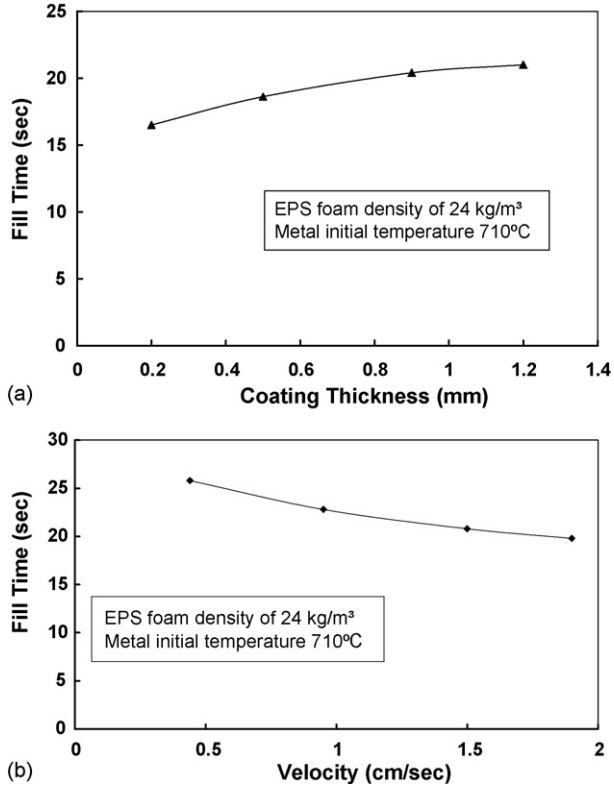

Fig. 6. Mold filling time as a function of (a) coating thickness; and (b) metal front velocity.

effect, the constant heat transfer coefficient in the basic model is modified by a correction factor, which is dependent on gas pressure and coating properties. The empirical correction factor to gas pressure and coating thickness is shown in Fig. 4. It can be seen that as coating thickness increases, the pressure correction factor decreases.

As shown in Fig. 5, the VHTC model with varying heat transfer coefficient dependent on the metal front pressure and orientation of gravity predicts the metal surface temperature better than the basic CHTC model with only gravity effect. Considering the experimental uncertainty shown in Fig. 5, good agreement is obtained between the VHTC model and experiment.

For the cylindrical geometry, a parametric study was performed for coating thickness and metal front velocity. Fig. 6(a) shows the mold fill time of the cylinder as a function of coating thickness. As the coating thickness increases, the heat transfer coefficient between the metal front and foam pattern decreases and the fill time increases. As the metal front velocity increases, the fill time decreases as shown in Fig. 6(b).

To further illustrate the improved model with pressure effect, a numerical simulation is performed for a simple plate (28 cm × 15 cm × 1.3 cm) with two side ingates and a top ingate. The computational domain is shown in Fig. 1(b) with $L = 28$ cm and $W = 15$ cm. The inlet height H is 12 cm. EPS foam of nominal density 20 kg/m^3 is used. No-slip boundary conditions are applied at the mold walls, and pressure boundary condition is applied at the inlet. The numerical model is compared with the experimental data of Shivkumar and Galois [18]. The experimental results of the metal front arrival times at different locations in the plate with hollow sprue and ingates are shown in Fig. 7(a). Computer simulation results from the basic CHTC model with gravity effect are shown in Fig. 7(b), and results from the VHTC model incorporating metal front pressure and coating effect are shown in Fig. 7(c). It is apparent that the CHTC model with only gravity effect is not sufficient to predict the times of metal filling locations. The metal front tends to move faster through the bottom-side gate than through the upper side gate and the top gate. The last place to fill in the plate is about 2 cm above the plate mid-height in the experiment that is almost the same as that predicted by the VHTC model, whereas the basic CHTC model with only gravity effect predicts that the last place to fill is at mid-height of the plate. Fig. 7(d)

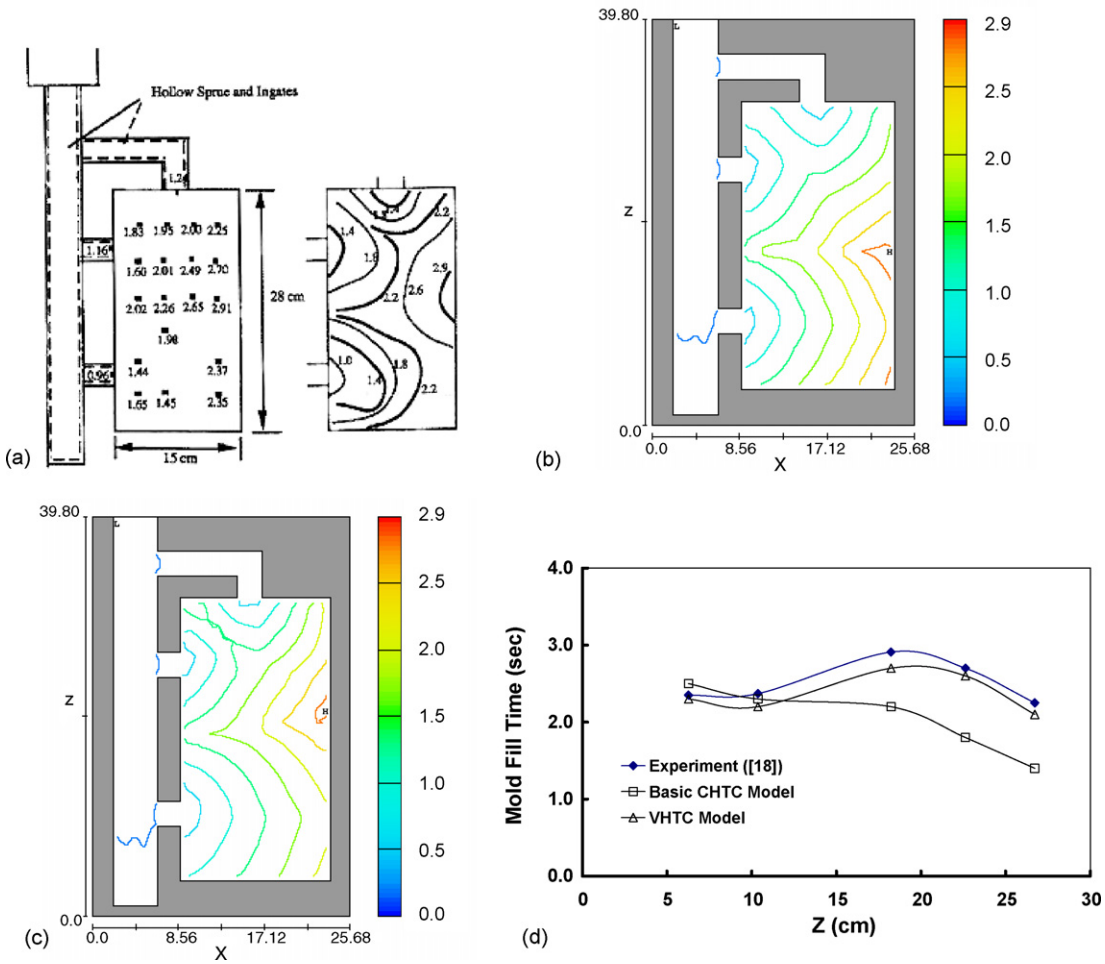

Fig. 7. Comparison of mold filling times for a plate pattern with three ingates: (a) measured values by thermometric technique [18]; (b) predicted filling times based on basic CHTC model with gravity effect; and (c) predicted filing times based on the VHTC model with heat transfer coefficient changing with gas pressure; (d) mold filling time at the right-and wall of the mold for the plate pattern with three ingates.

shows the mold filling time at the right side wall of the mold indicating better agreement with the VHTC model.

3.3. Effect of metal temperature

A plate pattern from Yao [14] was used to validate the VHTC temperature model. The plate pattern 20 cm × 15 cm × 1.3 cm was placed horizontally with a side ingate of 1.3 cm × 1.8 cm in cross section. The computational domain is shown in Fig. 1(c) with $L = 20$ cm and $W = 15$ cm. An effective metallostatic head of 28 cm was applied at the inlet boundary, and no-slip boundary condition is used at the mold walls. The effect of metal temperature on the mold filling behavior was studied by using several different molten liquids. The initial temperatures indicated are representative values for wax, Sn, Al, and Cu, 225 °C, 525 °C, 750 °C, and 1150 °C, respectively. In the cited experimental study the molten liquid was rapidly poured into the mold with preheated ladle. It was observed that inlet temperatures dropped about 35 °C from the initial temperature. For the four inlet temperatures of 190 °C, 490 °C, 715 °C and 1115 °C, the times of mold filling are shown in Fig. 8 from experimental results. The arrow represents the position of the ingate. The filling times are 4.05, 2.1, 2.7 and 3.15 s for the four different temperatures, respectively. The basic CHTC model cannot simulate the effect of metal temperature on the metal filling velocity. The results from VHTC simulation are shown in Fig. 9 for the four cases. It can be seen that the experimental filling sequence is captured by the simulation. The maximum filling speed at 490 °C corresponds to the peak volatilization of EPS foam. For temperatures under 490 °C, the degradation products consist mainly of viscous residue, which increases the resistance to the molten liquid. For temperatures above 490 °C, the volume of gases produced increases and mold filling speed is decreased to a certain extent dependent on the elimination of the foam products. Although the basic CHTC model could not simulate temperature effects, the VHTC model predict the mold filling time fairly close to experimental data as evidenced in Fig. 9(e), showing the mold filling time at the right-hand surface of the mold.

3.4. Defect prediction

For the plate with three ingates, the predicted locations where two surfaces met based on the defect scalar are different from the two models as shown in Fig. 10(a) and (b). Since the filling times

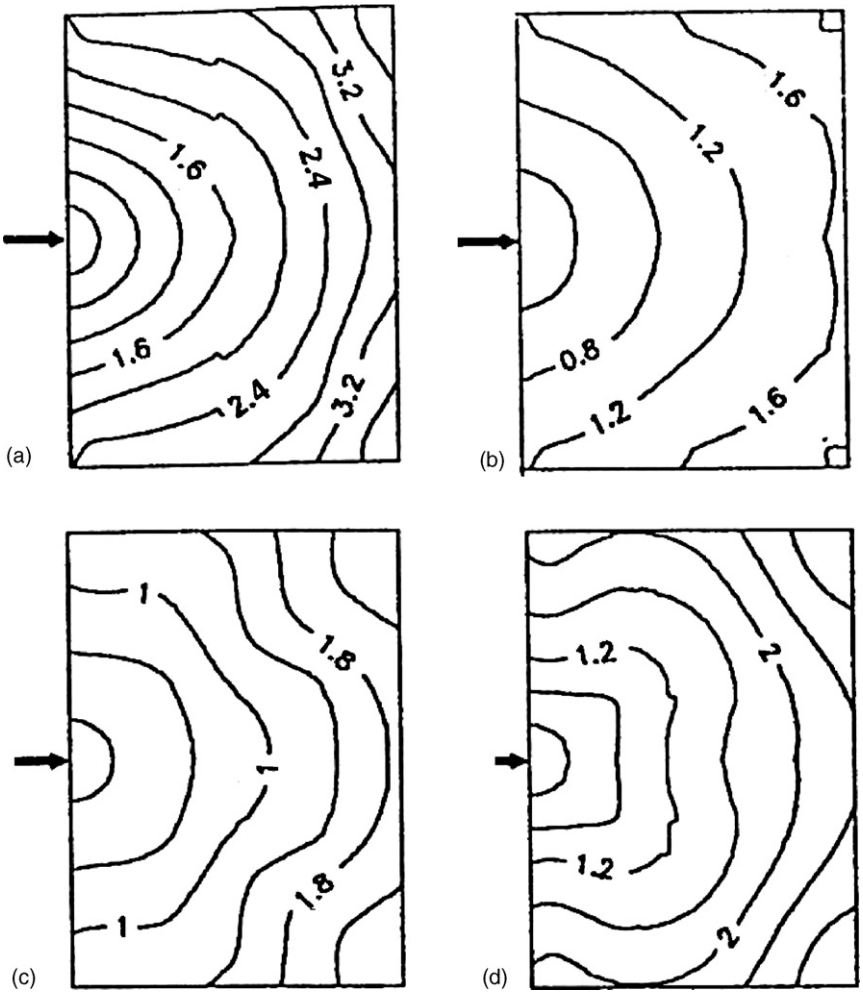

Fig. 8. Experimental results [14] showing the temperature effect on the mold filling times. The arrow represents the position of the ingate: (a) 190 °C; (b) 490 °C; (c) 715 °C; and(d) 1115 °C.

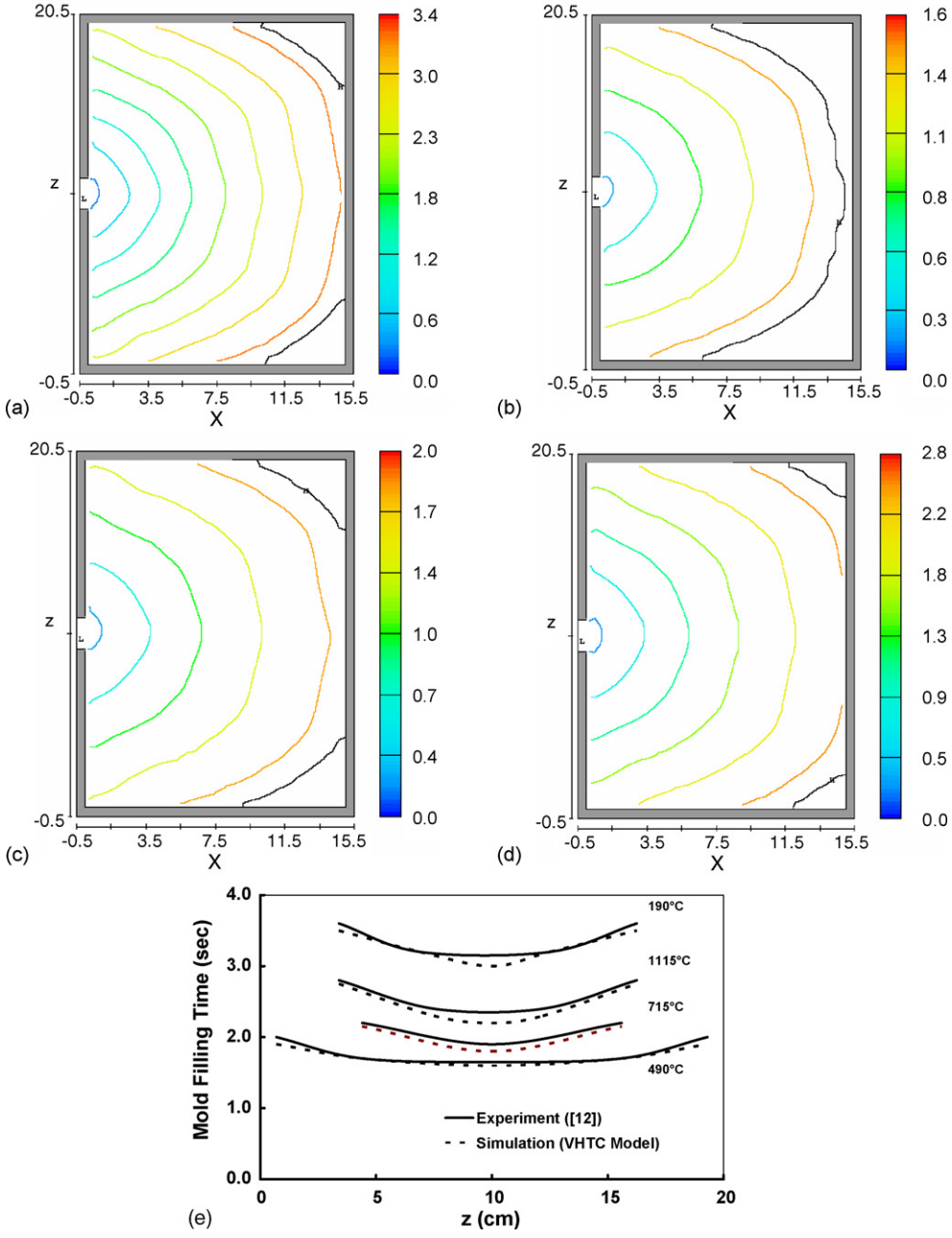

Fig. 9. Simulation results showing the temperature effect on the mold filling times. Color indicates time of filling (blue is earliest and red latest): (a) 190 °C; (b) 490 °C; (c) 715 °C; and (d)1115 °C; (e) mold filling time at the right side surface of mold showing the temperature effect.

are predicted more precisely by the VHTC model, it is concluded that more realistic defect formation is predicted by the VHTC model as shown in Fig. 10(b). One important observation is that there are many internal defects formed due to the meeting of two metal fronts predicted by the VHTC model. Because of the inclusion of gas pressure effect in the VHTC model, the defect near the bottom of the casting predicted in the basic model moves upwards into the casting and form internal defects.

The use of three ingates causes several metal fronts to meet during the mold filling process that leads to internal inclusions of foam products. To check if fewer gates can help reduce defects formation, a two-gate model is tested and shown in Fig. 10(c). The simulation results show that the defect at the right upper side of the casting is eliminated because of the removal of the top ingate. It is encouraging to see that the VHTC model provide considerable amount of useful insight into the processes responsible for defect formation and final distribution in a cast part. The defect model needs further experimental validation to correlate the predictions with actual defect formations; however, the model can reveal useful insight into the process variables that are responsible for defect generation and final distribution in castings.

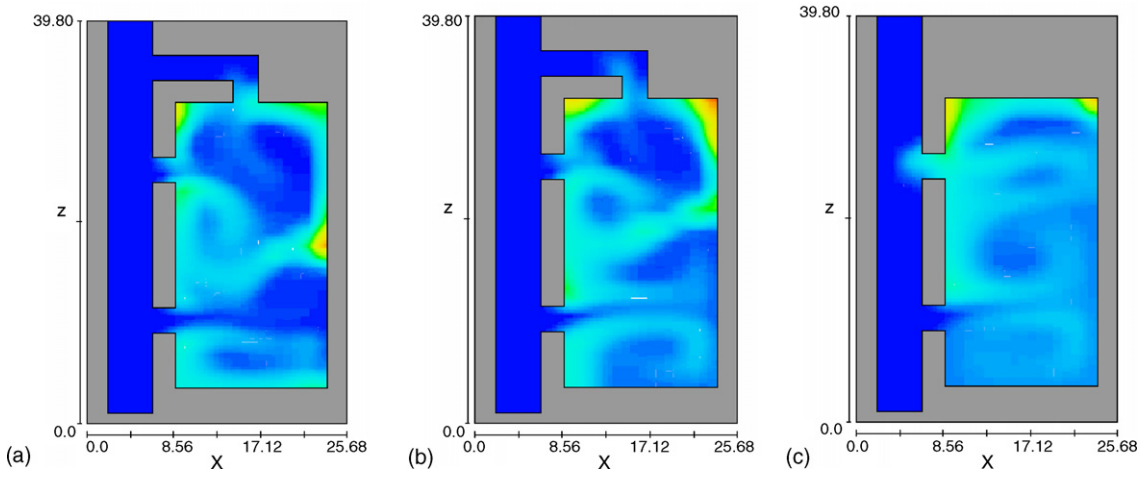

Fig. 10. Defects formation predicted by (a) basic CHTC model with gravity effect; (b) VHTC model with heat transfer coefficient based on both gas pressure and coating thickness; and (c) improved model for two ingates. Color represents probability for defects (blue is the lowest and red highest).

4. Conclusions

Computational modeling can be used to simulate combined effects of fluid flow, heat transfer and foam decomposition during the filling of the LFC process. By using the FAVOR method, a complex geometry can be modeled efficiently. An improved model incorporating a varying heat transfer coefficient, gas pressure, metal temperature, foam property and coating effects was developed to augment the user-defined subroutine. The simulation results from the VHTC model showed improved agreement with experimental observations and data reported in the literature. Metal front temperature was predicted within experimental uncertainty by the improved model, whereas the prediction made by the basic CHTC model had a much larger difference. Mold filling patterns and filling time difference of 1–4 s were more precisely captured by the improved model than the basic model for several geometries. The code can also be used to predict flow condition of molten metal, filling sequence, and defect formation for different geometries and process variables. This study provides additional insight into the effect of important process and design variables in what has traditionally been a very empirical field.

References

[1] S. Shivkumar, L. Wang, D. Apelian, The lost-foam casting of aluminum alloy components, JOM 42 (11) (1990) 38–44.
[2] M.H. Warner, B.A. Miller, H.E. Littleton, Pattern pyrolysis defect reduction in lost foam castings, AFS Trans. 106 (1998) 777–785.
[3] C.W. Hirt, B.D. Nichols, Volume of Fluid (VOF) method for the dynamics of free boundaries, J. Comp. Phys. 39 (1) (1981) 201–225.
[4] C. Wang, A.J. Paul, W.W. Fincher, O.J. Huey, Computational analysis of fluid flow and heat transfer during the EPC process, AFS Trans. 101 (1993) 897–904.
[5] Y. Liu, S.I. Bakhtiyarov, R.A. Overfelt, Numerical modeling and experimental verification of mold filling and evolved gas pressure in lost foam casting process, J. Mater. Sci. 37 (14) (2002) 2997–3003.
[6] S.M.H. Mirbagheri, H. Esmaeileian, S. Serajzadeh, N. Varahram, P. Davami, Simulation of melt flow in coated mould cavity in the lost foam casting process, J. Mater. Process. Technol. 142 (2003) 493–507.
[7] J.-H. Kuo, J.-C. Chen, Y.-N. Pan, W.-S. Hwang, Mold filling analysis in lost foam casting process for aluminum alloys and its experimental validation, Mater. Trans. 44 (10) (2003) 2169–2174.
[8] C.W. Hirt, Flow-3D User's Manual, Flow Science Inc., 2005.
[9] E.S. Duff, Fluid flow aspects of solidification modeling: simulation of low pressure die casting, The University of Queensland, Ph.D. Thesis, 1999.
[10] X.J. Liu, S.H. Bhavnani, R.A. Overfelt, The effects of foam density and metal velocity on the heat and mass transfer in the lost foam casting process, in: Proceedings of the ASME Summer Heat Transfer Conference, 2003, pp. 317–323.
[11] W. Sun, P. Scarber Jr., H. Littleton, Validation and improvement of computer modeling of the lost foam casting process via real time X-ray technology, in: Multiphase Phenomena and CFD Modeling and Simulation in Materials Processes, Minerals, Metals and Materials Society, 2004, pp. 245–251.
[12] T.V. Molibog, Modeling of metal/pattern replacement in the lost foam casting process, Materials Engineering, University of Alabama, Birmingham, Ph.D. Thesis, 2002.
[13] X.J. Liu, S.H. Bhavnani, R.A. Overfelt, Measurement of kinetic zone temperature and heat transfer coefficient in the lost foam casting process, ASME Int. Mech. Eng. Congr. (2004) 411–418.
[14] X. Yao, An experimental analysis of casting formation in the expendable pattern casting (EPC) process, Department of Materials Science and Engineering, Worcester Polytechnic Institute, M.S. Thesis, 1994.
[15] M.R. Barkhudarov, C.W. Hirt, Tracking defects, Die Casting Engineer 43 (1) (1999) 44–52.
[16] C.W. Hirt, Modeling the Lost Foam Process with Defect Predictions-Progress Report: Lost-Foam Model Extensions, Wicking, Flow Science Inc., 1999.
[17] D. Wang, Thermophysical Properties, Solidification Design Center, Auburn University, 2001.
[18] S. Shivkumar, B. Gallois, Physico-chemical aspects of the full mold casting of aluminum alloys, part II: metal flow in simple patterns, AFS Trans. 95 (1987) 801–812.